ECS Transactions, 3 (7) 443-450 (2006)
10.1149/1.2355842, copyright The Electrochemical Society

Analysis of Hole Transport in Arbitrarily Strained Germanium

G. Karlowatz, E. Ungersboeck, W. Wessner, H. Kosina, and S. Selberherr

Institute for Microelectronics, Technische Universität Wien
Gusshausstr. 27–29, 1040 Wien, Austria

Full-band Monte Carlo simulations are performed to study the properties of hole transport in bulk Germanium under general strain conditions. The band structures are calculated with the empirical non-local pseudopotential method. For Monte Carlo simulations acoustic and optical phonon scattering as well as impact ionization are taken into account. Results for biaxially strained Ge grown on a [001] oriented $Si_{1-x}Ge_x$ substrate and for uniaxial compressive stress in [110] exhibit a high mobility enhancement. These results are compared to experimental and theoretical results from literature.

Introduction

The history of semiconductor device technology started with Germanium as the preferred material, while today the mainstream semiconductor technology is centered around Silicon. Over decades performance gains and increasing integration density of CMOS devices where successfully obtained by down-scaling, a process which is getting more and more cost intensive as it is pushed closer to some principal physical limits. So the demand for alternatives to down-scaling rises, leading to new opportunities for Ge, particularly motivated by its higher carrier mobility compared to Si. The hole mobility, being approximately four times higher than in Si, can be further enhanced by stress engineering. This has been shown in previous experimental and theoretical works for biaxially strained Ge epitaxially grown on a [001] oriented Si_xGe_{1-x} substrate (1)(2)(3). In this work we analyze hole transport properties of arbitrarily stressed/strained Ge by means of full-band Monte Carlo simulation (FBMC).

Band Structure Calculation

For FBMC simulations a numerical representation of the band structure in the unit cell of the reciprocal lattice, the so-called *Brillouin zone*, is used to capture the dependence of the carrier energy on the wave vector. Because of symmetry only a part of the Brillouin zone - the *irreducible wedge* - has to be considered for band structure calculation. The volume of the irreducible wedge is determined by the number of symmetry elements $\mathrm{P}(\Gamma)$ at the center of the Brillouin zone of the strained lattice via $\Omega_{\mathrm{irred}} = \Omega_{\mathrm{BZ}}/\mathrm{P}(\Gamma)$. For the diamond type lattice of relaxed Ge $\mathrm{P}(\Gamma)$ is 48, for stress along $\langle 100\rangle, \langle 111\rangle$, and $\langle 110\rangle$, as shown in Fig. 1, $\mathrm{P}(\Gamma)$ is 16, 12, and 8, respectively, while for stress along arbitrary direction the lattice is invariant only to inversion, thus $\mathrm{P}(\Gamma) = 2$.

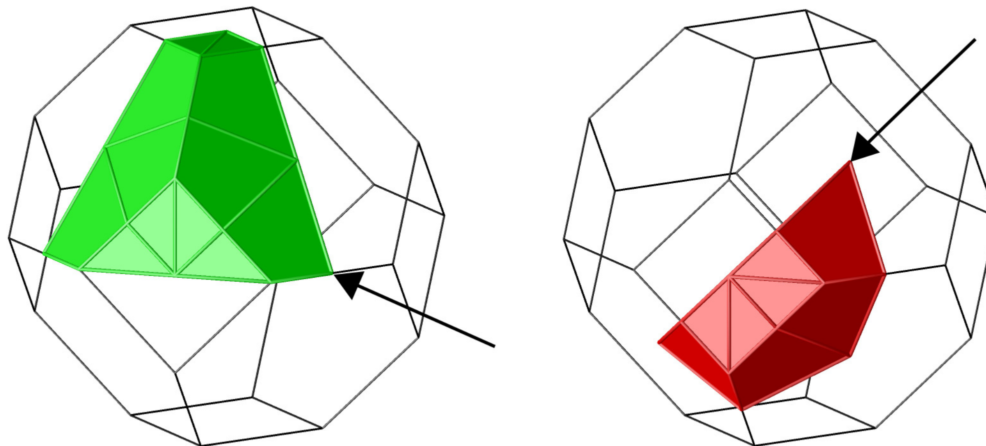

Fig. 1: Irreducible wedge for stress applied in [110] and in [111] direction.

The empirical non-local pseudopotential method (EPM) (4) is generalized to arbitrary stress/strain conditions to calculate the band structures of Ge. For discretization of the band-structure an unstructured tetrahedral mesh is used. Mesh refinement guarantees high resolution around the band minima, while a relatively low total number of mesh elements is maintained (5).

Stress modifies the band structure of a semiconductor. As a consequence the band gap changes, a splitting between light hole and heavy hole band is introduced and also the splitoff band is altered. The band splitting reduces the density of states in the low energy regime and suppresses interband scattering. This effect and the change of the effective masses cause the observed mobility gain. Fig. 2(a) shows the energy splitting between the splitoff band and the valence band edge and Fig. 2(b) the heavy/light hole band splitting energies of biaxially strained Ge grown on a [001] oriented $Si_{1-x}Ge_x$ substrate as a result of EPM calculation (4). For higher compressive strain levels than shown the heavy/light hole band splitting saturates (1). Fig. 3(a)

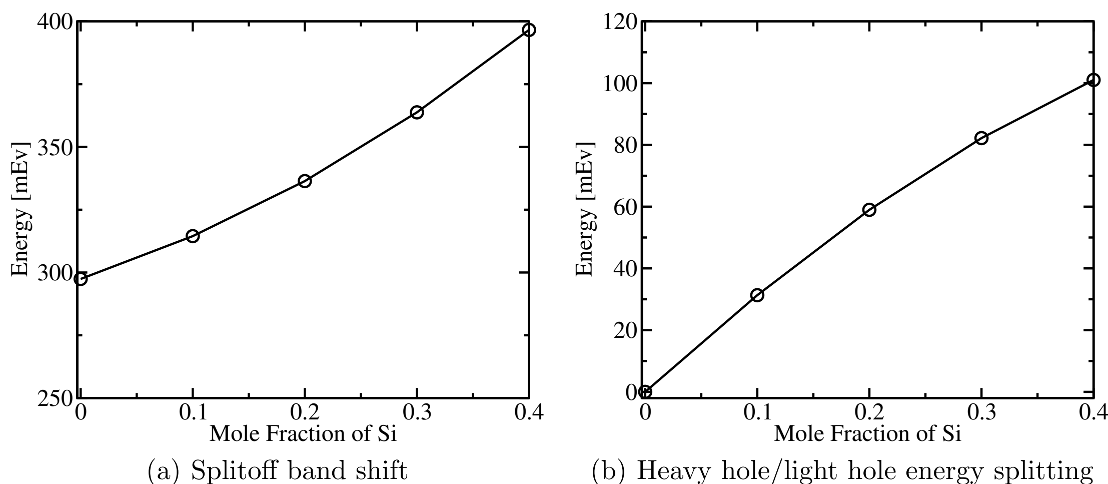

(a) Splitoff band shift

(b) Heavy hole/light hole energy splitting

Fig. 2: Splitoff band shift and heavy hole and energy splitting of heavy hole/light hole bands in strained Germanium grown on a Si_xGe_{1-x} layer.

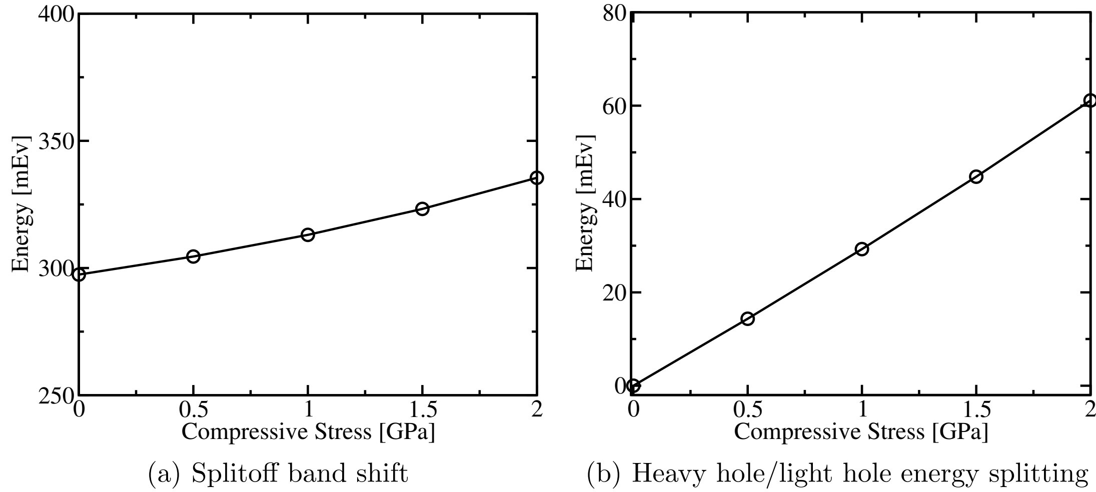

(a) Splitoff band shift (b) Heavy hole/light hole energy splitting

Fig. 3: Splitoff band shift and heavy hole and energy splitting of heavy hole/light hole bands of stressed Ge with compressive stress in [110] direction.

depicts the energy splitting between the splitoff band and the valence band edge and Fig. 3(b) the heavy/light hole band splitting energies of compressive stressed Ge in [110] direction. The splitting energy rises almost linearly with compressive stress in [110] direction for the shown range of pressure.

The Vienna Monte Carlo Simulator

The Vienna Monte Carlo Simulator (VMC) (6) offers simulation algorithms for both bulk semiconductors and one-dimensional devices based on analytical and full-band models. Additionally, a fast zero-field algorithm is included (7). VMC provides a mature set of scattering models including phonon scattering, ionized impurity scattering, alloy scattering, and impact ionization. For full-band simulation phonon scattering models with constant matrix elements are used(8). In this formulation the scattering rates are proportional to the density of states, which is calculated from the band structure. The coupling constants for acoustic and optical phonon scattering, as well as the optical phonon energy are given in Table 1. These parameters are used for relaxed and for strained Ge. Impact ionization is modeled with a threshold expression (9)

$$\frac{1}{\tau_{\mathrm{ii}}} = \theta(\epsilon - \epsilon_{\mathrm{th}}) \cdot \mathrm{P} \cdot \left(\frac{\epsilon - \epsilon_{\mathrm{th}}}{\epsilon_{\mathrm{th}}}\right)^{3.5} \qquad [1]$$

where θ is the unit step-function, ϵ is the electron energy, ϵ_{th} is a threshold energy, and P is a multiplication factor which determines the softness of the threshold. The parameters are tuned to reproduce reported hole velocity field characteristics (10)(11)(12) for relaxed Ge, $\epsilon_{\mathrm{th}} = 0.69\mathrm{eV}$ and $\mathrm{P} = 2.0 \cdot 10^{12}\mathrm{s}^{-1}$. For stressed/strained Ge ϵ_{th} is adjusted in dependence on the bandgap change.

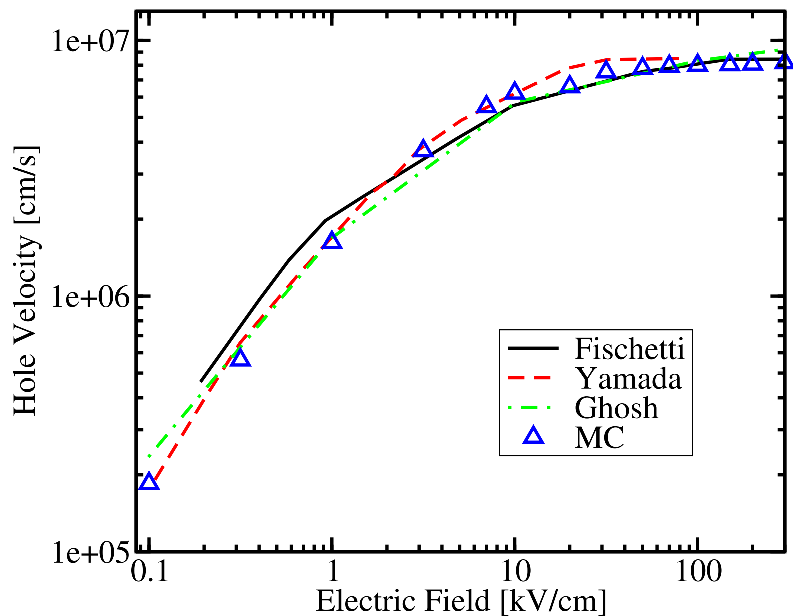

Fig. 4: Hole velocity versus field in [100] direction for relaxed Ge compared to results from literature.

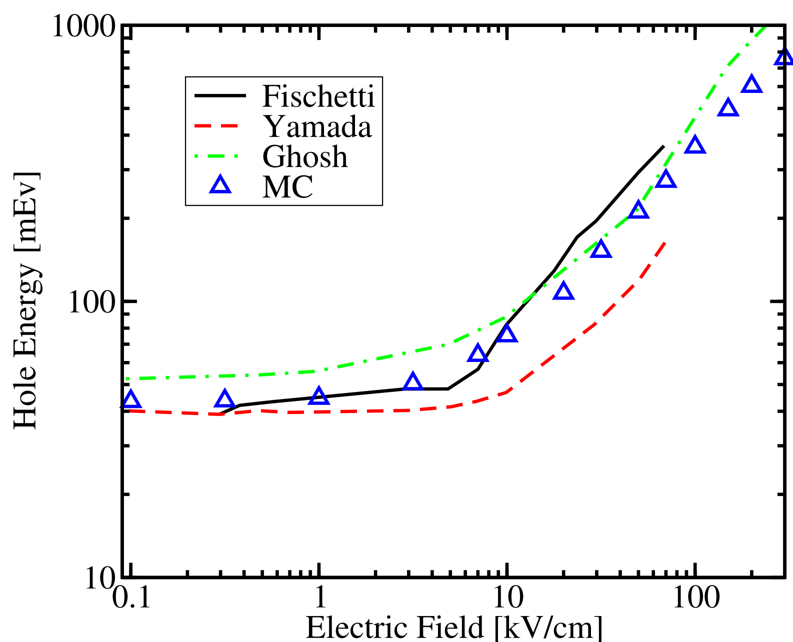

Fig. 5: Hole energy versus field in [100] direction for relaxed Ge compared to results from literature.

Fig. 4 shows the hole velocity field characteristics and Fig. 5 the energy as a function of the electric field in [100] direction for relaxed Ge. These results are compared to values from literature and show good agreement.

Table 1: Acoustic deformation potential Δ_{ac}, optical deformation potential Δ_{op} and optical phonon energy $\hbar\omega_{op}$ for the heavy hole (HH), light hole(LH) and split-off (SO) bands.

Band	Δ_{ac}	Δ_{op}	$\hbar\omega_{op}$
HH	1.71 eV	9.6e8 eV/cm	37 meV
LH	2.56 eV	9.6e8 eV/cm	37 meV
SO	2.56 eV	9.6e8 eV/cm	37 meV

Results

Compressively Biaxially Strained Germanium

In this section simulation results for bulk hole transport in biaxially strained Ge epitaxially grown on a $\mathrm{Si}_x\mathrm{Ge}_{1-x}$ substrate with [001] orientation are shown. Since the lattice constant of SiGe is smaller than that of Ge the resulting strain is compressive. Several pMOSFET devices with strained Ge channels based on that technique have been demonstrated (2)(3).

Fig. 6 depicts the in-plane low field mobility versus mole fraction of Si in the $\mathrm{Si}_x\mathrm{Ge}_{1-x}$ substrate. For a mole fraction $x = 0.4$ the low field hole mobility is enhanced by a factor of 3.38 to 6350 $\mathrm{cm}^2/\mathrm{Vs}$. This mole fraction corresponds to biaxial compressive strain of 1.7% in the Ge layer. Fig. 7 shows the velocity field characteristics for field in [100] direction for different Si mole fractions. The highest mobility gain can be observed in the low field regime, while the curves converge in the high field regime.

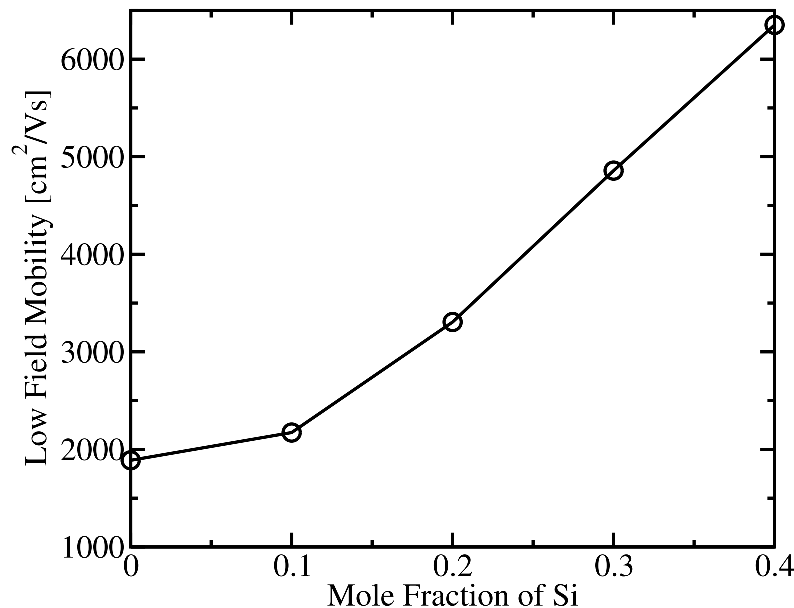

Fig. 6: In-plane low field mobility of holes in biaxially compressed Ge grown on a $\mathrm{Si}_x\mathrm{Ge}_{1-x}$ substrate.

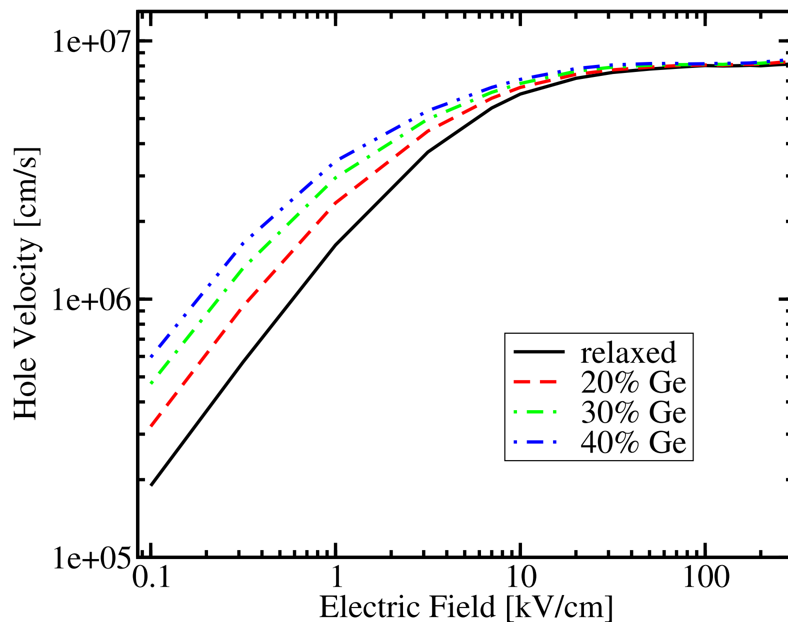

Fig. 7: Hole velocity versus electric field for biaxially compressed Ge grown on a Si_xGe_{1-x} substrate in [100] direction.

Uniaxially Strained Germanium

Uniaxial stress technique overcomes a few drawbacks of biaxially strained Ge layers, related to problems of misfit and threading dislocations as well as diffusion. In

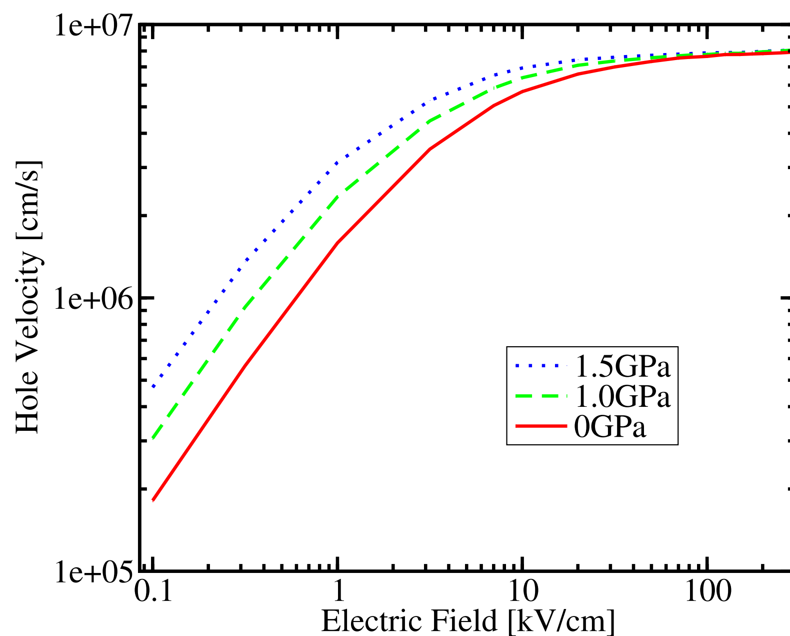

Fig. 8: Hole velocity as a function of the electric field in stressed Ge for field and stress in [110] direction.

Si technology CMOS devices with uniaxially stressed channels are already fabricated in large volumes (13). The stress is hereby introduced by capping layers. In this section results for hole transport in uniaxially stressed Ge with compressive stress in [110] are shown. Although this is a technologically very interesting setup it has been hardly investigated by means of Monte Carlo simulation so far.

Fig. 8 presents the velocity field characteristics for uniaxial stress and field in [110] direction. As for biaxially strain the curves show the highest mobility gain in the low field regime and converge at high electric fields.

Fig. 9 depicts the in-plane hole mobility at low electric field for uniaxial compressive stress. A strong anisotropy with the most pronounced mobility enhancement in stress direction can be observed. A stress level of 1.5GPa enhances the low field mobility by a factor of 2.55 to 4790 cm^2/Vs. Note that tensile stress instead of compressive stress could also be used for hole mobility enhancement. The most pronounced enhancement is then achieved perpendicular to the applied stress in$[\bar{1}10]$ direction, otherwise the result looks similar as in Fig. 9 for the shown stress levels.

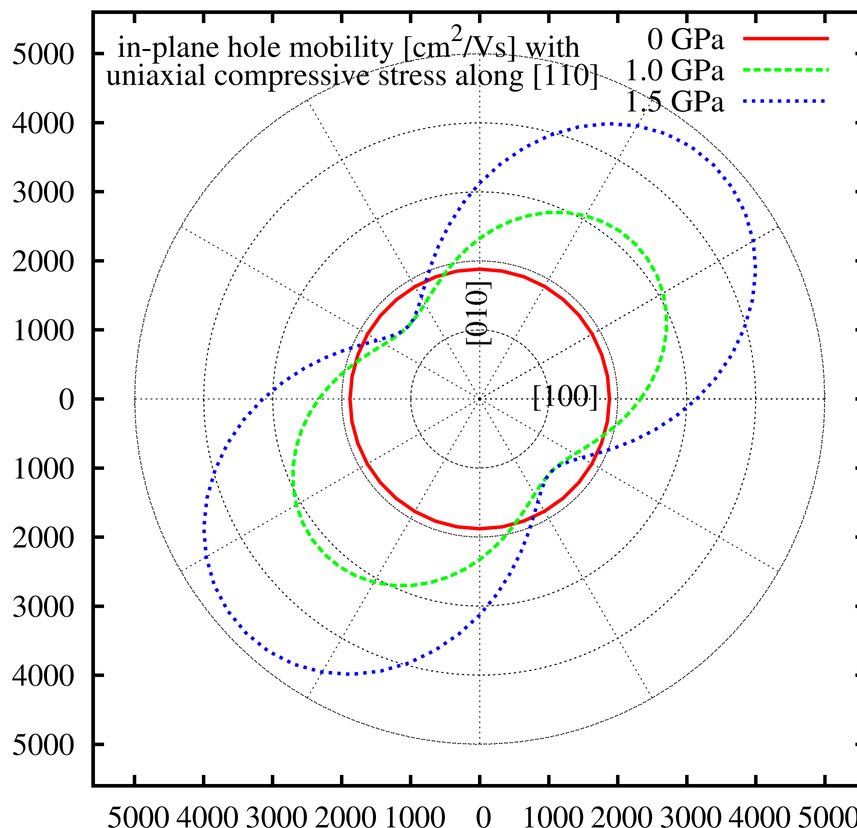

Fig. 9: Low field hole mobility in bulk Ge for uniaxial [110] compressive stress.

Conclusion

A full-band Monte Carlo simulator which efficiently handles arbitrary stress/strain conditions is presented and used to analyse two technologically important applications of stress engineered Ge. It is demonstrated that uniaxial compressive stressed Ge in [110] direction as well as biaxially stressed Ge show high hole mobility enhancement. Therefore, Germanium is indeed a promising material for future applications.

Acknowledgment

This work has been partly supported by the Austrian Science Fund, contract F2509-N08.

References

1. M. V. Fischetti and S. Laux, *J. Appl. Phys.*, **80**, 2234 (1996).
2. M. L. Lee, C. W. Leitz, Z. Cheng, A. J. Pitera, T. Langdo, M. T. Currie, G. Taraschi, E. A. Fitzgerald, and D. A. Antoniadis, *Appl. Phys. Lett.*, **79**(20), 3344 (2001).
3. A. Ritenour, S. Yu, M. L. Lee, N. Lu, W. Bai, A. Pitera, E. A. Fitzgerald, D. L. Kwong, and D. A. Antoniadis, *IEDM Tech. Dig.*, 433 (2003).
4. M. Rieger and P. Vogl, *Phys. Rev. B*, **48**, 14276 (1993).
5. G. Karlowatz, W. Wessner, and H. Kosina, *Mathmod*, **1**, 316 (2006).
6. Institute for Microelectronics, VMC 2.0 User's Guide, TU Wien, http://www.iue.tuwien.ac.at/software/vmc (2006).
7. S. Smirnov, H. Kosina, M. Nedjalkov, and S. Selberherr, *Lecture Notes in Computer Science*, p. 185, Springer, (2003).
8. C. Jacoboni and L. Reggiani, *Rev. Mod. Phys.* **55**, 645 (1983).
9. E. Cartier, M. V. Fischetti, E. A. Eklund, and F. R. McFeely, *Appl. Phys. Lett.*, **62**, 3339 (1993).
10. S.M. Sze, *Physics of Semiconductor Devices*, p. 47, Wiley, New York (1981).
11. T. Yamada and D. K. Ferry, *Solid State Electron.*, **38**, 881 (1995).
12. B. Ghosh, X. F. Fan, and L. F. Register, *IEEE Transactions on Electr. Devices*, **53**(3), 533 (2006).
13. T. Ghani, M. Armstrong, C. Auth, M. Bost, P. Charvat, T. Hoffmann, K. Johnson, C. Kenyon, J. Klaus, B. McIntyre, K. Mistry, J. Sandford, M. Silberstein, S. Sivakumar, P. Smith, K. Zawadzki, S. Thompson, and M. Bohr, *IEDM Tech. Dig.*, 978 (2003).